

# Second-harmonic generation as probe for structural and electronic properties of buried GaP/Si(001) interfaces

K. Brixius,<sup>1</sup> A. Beyer,<sup>1</sup> J. Gdde,<sup>1</sup> M. Drr,<sup>2</sup> W. Stolz,<sup>1</sup> K. Volz,<sup>1</sup> and U. Hfer<sup>1</sup>

<sup>1</sup>*Fachbereich Physik und Zentrum fr Materialwissenschaften,  
Philipps-Universitt, D-35032 Marburg, Germany*

<sup>2</sup>*Institut fr Angewandte Physik, Justus-Liebig-Universitt Gießen, D-35392 Gießen, Germany*  
(Dated: April 22, 2022)

Optical second-harmonic generation is demonstrated to be a sensitive probe of the buried interface between the lattice matched semiconductors gallium phosphide and silicon with (001) orientation. Rotational anisotropy measurements of SHG from GaP/Si show a strong isotropic component of the response not present for pure Si(001) or GaP(001). The strength of the overlaying anisotropic response directly correlates with the quality of the interface as determined by atomically resolved scanning transmission electron microscopy. Systematic comparison of samples fabricated with different growth modes in metal organic vapor phase epitaxy reveals that the anisotropy for different polarization combinations can be used as a selective fingerprint for the occurrence of anti-phase domains and twins. This all-optical technique can be applied as an *in-situ* and non-invasive monitor even during growth.

The investigation of interfacial properties is one of the most challenging tasks in modern material science and engineering of electronic devices. Within the last few years large efforts have been made on the structural analysis of interfaces by means of crosssectional scanning tunneling microscopy, atomic force microscopy or scanning transmission electron microscopy (STEM). The latter technique is particularly suited for this purpose because it can yield element specific information about interfaces of inorganic materials with atomic resolution. However, all these methods require a subsequent invasive preparation of the samples in order to access the interface in *ex situ* experiments.

In contrast to these methods, all-optical techniques allow a non-invasive *in situ* access to interfaces, which is basically only limited by the optical absorption length of the investigated material system. Moreover, even order nonlinear optical techniques such as second harmonic generation (SHG) intrinsically have a high interface sensitivity owing to the symmetry breaking at the crystal surface and at interfaces. [1–4] The interface sensitivity is particularly high for centrosymmetric materials where the bulk second-order susceptibility  $\chi^{(2)}$  vanishes in dipole approximation. However, even in non-centrosymmetric polar materials with strong nonlinear bulk response such as GaAs or GaP, high interface sensitivity can be achieved by suppressing the bulk response for particular polarization combinations of the incoming fundamental and generated second-harmonic light. [5, 6]

Here, we combine STEM and SHG to investigate the interface between the III/IV-material gallium phosphide and silicon which represents a model system for the growth of a polar on a non-polar material and which promises many application for optoelectronic applications based on silicon electronics. [7, 8] This system is of particular interest because the lattice mismatch between GaP(001) and Si(001) is small. Therefore, strain induced defects can be neglected. Nevertheless, the heteroepitaxial growth is challenging because the interface is

not automatically charge neutral and anti-phase domains (APDs) can be formed at monoatomic steps of the substrate. [9, 10] Moreover, stacking faults and twins can be formed in the GaP film. The latter occur if a part of the crystal is rotated with respect to the main crystal orientation. The structure of these defects have been extensively investigated by means of STEM. [11–13] In order to optimize the conditions for a defect-free growth, however, an *in situ* technique for the evaluation of the interface quality during growth would represent a great progress towards an detailed understanding of the interface formation and for the preparation of highly efficient devices.

In this letter we show that SHG is able to non-invasively investigate the properties of the buried interface between GaP and Si and that it possible to directly relate the SHG anisotropy to the film quality. For this purpose we have prepared GaP/Si samples by metal organic vapor phase epitaxy (MOVPE) under different growth conditions that give rise to specific defects such as ADPs and twins. We present sets of the rotational anisotropy of the second harmonic intensity for different polarization combinations of the incoming fundamental and generated second harmonic in reflection and compare these results with atomically resolved STEM measurements. The combination of both experimental techniques allow us to identify the occurrence of the specific defects in the second harmonic anisotropy of particular polarization combinations. This makes it feasible to use second-harmonic anisotropy as an *in situ*, non-invasive probe for the interface quality even during growth.

The experiments were performed under ambient conditions using 50 fs laser pulses generated by a femtosecond Ti:Sapphire laser amplifier system operating at 800 nm with a repetition rate of 15 kHz. The linear polarized laser beam at fundamental frequency  $\omega$  was focussed under an angle of  $45^\circ$  onto the sample as is illustrated in Fig.1 a). The generated second harmonic (SH) light at frequency  $2\omega$  was observed in reflection for a chosen

combination of input and output polarization, e.g.  $p$ -polarized incident light and  $s$ -polarized  $2\omega$ -light (abbreviated by  $pS$ ). Standard boxcar-integrator-technique was used for detection as described in detail in Ref. 14. The SH signal has been normalized with respect to a reference that was generated in a quartz crystal in  $pP$  configuration. The rotational anisotropy of the SH intensity was measured by rotating the sample around the surface normal ( $z$ -axis) as characterized by the azimuthal angle  $\Psi$ . The samples were oriented such that for  $\Psi = 0^\circ$  ( $180^\circ$ ) the  $[\bar{1}10]$ - ( $[1\bar{1}0]$ )-direction was lying within the plane of incidence (cf. Fig.1 a)). The fluence of the incident laser radiation was kept at least one order of magnitude below  $100 \text{ mJ/cm}^2$  which we determined as the threshold for multishot damage of our samples.

The investigated GaP-layers were grown by metal organic vaporphase epitaxy (MOVPE) in an Aixtron AIX 200 GFR reactor using triethylgallium (TEGa) and tertiary-butyl phosphine (TBP) as precursors for gallium and phosphorus, respectively. Four samples were prepared by using flow rate modulated epitaxy (FME), for which TEGa and the TBP were supplied intermittently in a total of sixteen cycles, starting with TEGa. The supply of GaP per cycle was varied between 0.2 to 1.36 monolayer by a variation of the partial pressure of TEGa between  $7.6 \times 10^{-4}$  mbar and  $7.6 \times 10^{-3}$  mbar while holding the TBP pressure constant at 0.91 mbar. In the following, these samples are referred to as FME0.20ML and so forth. For one sample, the continuous growth mode (CGM) was used, in which TEGa and TBP were applied simultaneously. The total thickness of the layers varied between 0.8 and 4.5 nm as was determined by X-ray reflection in a X'Pert Pro diffractometer. Complementary characterization was carried out in a JEOL 2200FS scanning transmission electron microscope (STEM) operating at 200 kV. This STEM can achieve atomic resolution in the high angle annular darkfield imaging mode by aberration corrections of the probe forming lenses.

The azimuthal dependence of the SH intensity for all samples and polarization combinations is presented in Fig. 1 (b)-(h). These rotation patterns offer a direct access to the symmetry and rotational anisotropy of the second-order nonlinear response. [3] For the GaP wafer (Fig. 1 (g)), a four-fold anisotropy was found for the polarization combinations  $pP$ ,  $pS$  and  $sP$  as is consistent with other reports. [5] This anisotropy results from the  $\bar{4}3m$ -symmetry group for zincblende crystals and is a pure bulk dipole contribution. The  $pS$ -combination shows the strongest SHG; it vanishes completely if the polarization of the fundamental is along the  $[110]$ - and  $[\bar{1}\bar{1}0]$ -direction. Compared to the GaP wafer, the SH response of the native oxide covered Si(001) wafer (Fig. 1 (h)) is weaker by about four orders of magnitude. Its fourfold anisotropy is known to originate from the bulk quadrupole contribution [15] whereas the isotropic contribution is attributed to the  $\text{SiO}_2$  layer or the  $\text{Si/SiO}_2$  interface. [16] Within our detection limit, no SH signal could be observed for the combination  $sS$  for both the GaP and the Si wafer.

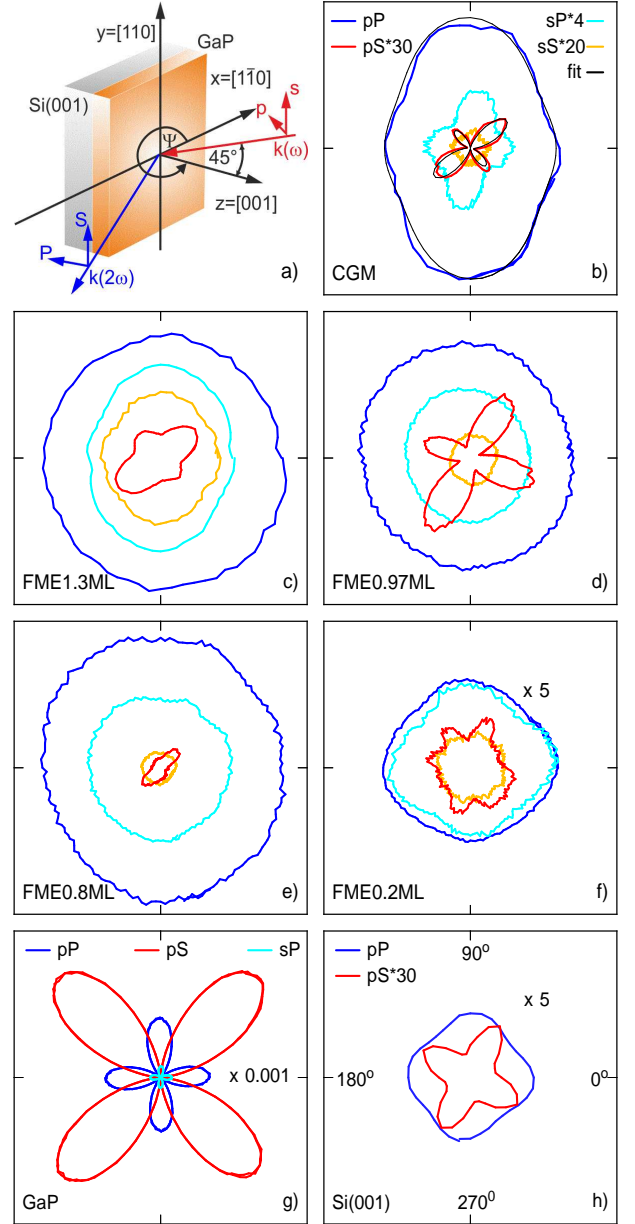


FIG. 1: (Color online) (a) Experimental setup. (b)-(f) Polar plots of the rotational SH anisotropy from five different GaP/Si(001) samples for different polarization combinations of the incoming fundamental and the detected SH as denoted in (b). For comparison, (g) and (h) show the signal of a GaP(001) wafer and a Si(001) wafer, respectively. The signals of the different polarization combinations have been scaled as denoted in the different figures for better comparison. Black lines in (a) exemplarily show fits of Eq. 1 for the combinations  $pP$  and  $pS$ , respectively.

Compared to the wafers, the SH response of the five heteroepitaxially grown films of GaP on Si(001) (Figs. 1 (b)-(f)) differs remarkably, both in overall intensity and in particular in anisotropy. Most prominent is the dominant isotropic contribution in the patterns for the  $pP$

(blue lines) and the  $sP$  (cyan lines) polarization combination. Except for the thinnest sample FME0.2ML, this signal is considerably larger as compared to the response of the Si wafer. Moreover, it by far outreaches the almost invisible four-fold anisotropic bulk contribution of the GaP films. We therefore exclude surface contributions and assign this isotropic signal to the interface between GaP and Si. This is supported by additional measurements for GaP layer with thicknesses of up to 65 nm (not shown) which showed that the isotropic contribution of the SH response decreases exponentially with the GaP layer thickness.

A second-order nonlinear response of the interface between two semiconductors can arise either from the presence of a static electric field due to the band alignment of both materials [17] or from the modification of the chemical bonds at the interface. The latter is here related to the hybridized  $sp^3$  orbitals that are distorted due to the Ga-Si and P-Si bonds. Similar, although quantitatively stronger effects, have been observed for the clean Si surface, where a comparable symmetry break due to surface reconstruction results in an increase of the SH intensity by a factor of  $\sim 100$ . [18] In the case of the GaP/Si interface, it increases compared to the oxidized Si surface by only a factor of about ten. This weaker effect might be connected to a cancelation due to bond distortions in opposite directions. An electric field at the interface gives rise to the EFISH-effect [19, 20], which also predominantly contributes to the p-polarized component of the SH intensity because it particularly affects the nonlinear response perpendicular to the interface. It has been demonstrated that fields due to depletion layers can even exceed the nonlinear bulk response. [6, 21–23] Most probably both distorted bonds and EFISH contribute to this isotropic interface response.

The  $pS$  contribution (red curves in Fig.1) of the SH response seems to be less affected by the interface because its shape is similar to the response of the Si and the GaP wafer. Its strength, however, is almost five orders of magnitude smaller as compared to the bulk response of the GaP wafer. This is surprising because the penetration depth of the fundamental light  $\delta_{\text{GaP},800\text{nm}}$  is about 160  $\mu\text{m}$  and the SH intensity increases up to a film thickness of  $\sim 30$  nm before a reduction due to a phase shift between the  $\omega$  and  $2\omega$  light sets in. Therefore, the GaP bulk contribution from thin films of a few nm thickness should only be smaller by about one order of magnitude compared to the thick wafer. This strong reduction of the bulk response is most likely being caused by a destructive interference due the appearance of antiphase domains because the phase of the SH response originating from P-polar GaP is shifted by about  $\pi$  in comparison to the response of the Ga-polar GaP. [24]

Beyond these general differences between the SH response of the native wafers and the GaP/Si heterostructures, the different samples show characteristic variations for all measured polarization combinations. In the following we show that these individual differences of the

SH response can be related to structural differences that have been obtained by STEM. This makes it possible to use the nonlinear response as a fingerprint for the GaP/Si interfaces and even distinguish between different growth modes within MOVPE.

For this purpose a symmetry analysis has been applied that quantifies the different isotropic and anisotropic contributions to the nonlinear response. Phenomenologically, the second-harmonic intensity in reflection for a given polarization combination  $ij$  can be written as a function of the incidence intensity  $I_i(\omega)$  as  $I_{ij}(2\omega) \propto |\chi_{\text{eff},ij}^{(2)}|^2 I_i^2(\omega)$  where  $\chi_{\text{eff},ij}^{(2)}$  is an effective second-order nonlinear susceptibility tensor of third rank that includes all contributions (surface, interface, bulk, EFISH etc.) to the second-order nonlinear polarization [3] even if the intrinsic material response of the bulk and EFISH contributions might be in the most general case described by higher-order tensors of the nonlinear susceptibility [20, 25]. The dependence of  $I_{ij}(2\omega)$  on the azimuthal angle  $\Psi$  can be then written as a Fourier expansion up to the fourth order

$$I_{ij}(2\omega) \propto \left| a_{ij} + \sum_{m=1}^4 b_{ij}^{(m)} \cos m\Psi + c_{ij}^{(m)} \sin m\Psi \right|^2, \quad (1)$$

where the isotropic ( $a_{ij}$ ) and anisotropic coefficients ( $b_{ij}^{(m)}$ ,  $c_{ij}^{(m)}$ ) contain all optical properties, in particular the corresponding components of the nonlinear susceptibility tensors as well as Fresnel coefficients. For (001) oriented samples, odd orders  $m$  can be excluded.

Table I lists the expected non-vanishing isotropic and anisotropic coefficients at the different polarization combinations for all considered SHG sources, i.e. Si-surface, -bulk and -EFISH as well as GaP-bulk and -EFISH.

Within this model the azimuthal dependence of the SH intensity can be well described for all polarization combinations by a least-square fit of the coefficients  $a_{ij}$ ,  $c_{ij}^{(2)}$ ,  $b_{ij}^{(2)}$  and  $b_{ij}^{(4)}$ , i.e. omitting the  $c_{ij}^{(4)}$ . The black lines in Fig. 1 (b) shows two exemplary examples of these fits for the polarization combinations  $pP$  and  $pS$ .

Figure 2 summarizes the fitting results for the polarization combinations  $pP$ ,  $pS$ , and  $sS$ . For all heterostructures

origin of SHG	$pP$	$pS$	$sP$	$sS$
Si (single-domain)	$a_{pP}, c_{pP}^{(2)}$	$b_{pS}^{(2)}$	$a_{sP}, c_{sP}^{(2)}$	–
Si (multi-domain)	$a_{pP}$	–	$a_{sP}$	–
Si bulk	$a_{pP}, c_{pP}^{(4)}$	$b_{pS}^{(4)}$	$a_{sP}, c_{sP}^{(4)}$	$b_{sS}^{(4)}$
Si EFISH $\chi^{(3)}$	$a_{pP}$	–	$a_{sP}$	–
GaP bulk	$b_{pP}^{(2)}$	$c_{pS}^{(2)}$	$b_{sP}^{(2)}$	–
GaP quadrupole	$a_{pP}, c_{pP}^{(4)}$	$b_{pS}^{(4)}$	$a_{sP}, c_{sP}^{(4)}$	$b_{sS}^{(4)}$
GaP EFISH $\chi^{(3)}$	$a_{pP}$	–	$a_{sP}$	–
GaP EFISH $\chi^{(4)}$	$b^{(2)}$	$c^{(2)}$	$b_{sP}^{(2)}$	–

TABLE I: Isotropic and anisotropic contributions to the SHG from bulk, surface and EFISH of Si(001) and GaP(001).

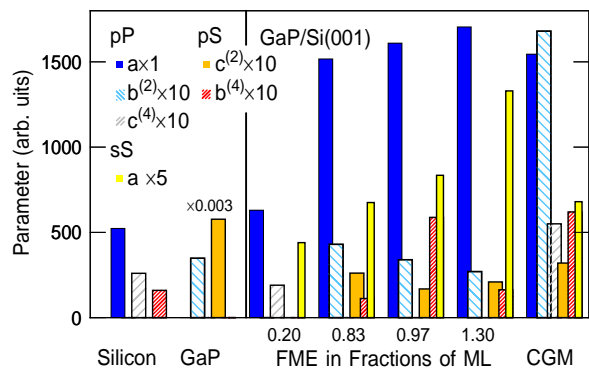


FIG. 2: (Color online) Isotropic and anisotropic coefficients for all investigated samples as obtained by a least-square fit of Eq. 1 for the polarization combinations  $pP$ ,  $pS$ , and  $sS$ .

tures the interface specific isotropic parameter  $a_{pP}$  (blue bars) dominates the total response. For the sample with the smallest GaP thickness of 0.8 nm (FME0.20ML), the magnitude of this contribution is comparable to that of the Si wafer. For the other GaP/Si samples, including the CGM sample,  $a_{pP}$  shows only a small variation. This suggests that the interface properties do not change strongly for GaP layer thicknesses of 1.6-4.5 nm.

The STEM images show, however, that the number of defects in the interface-near region of the FEM samples increases substantially for a GaP supply of more than 1 ML per cycle. This can be clearly seen by comparing the STEM images of FEM0.97ML and FEM1.30ML in Fig. 3 (a) and (c), respectively. Whereas the GaP film of sample FEM0.97ML shows no visible defects and a rather abrupt interface, two APDs of opposite polarity can be identified in the left and right part of the STEM image of sample FEM1.30ML. These APDs form if an excess of TEGa pressure etches Ga droplets into the Si crystal which then serve as nuclei for APDs. [26] The formation of APDs causes an in-plane symmetry reduction that affects predominantly the in-plane ( $s$ -polarized) SHG components. This is directly reflected by the strong increase of the isotropic  $a_{sS}$  contribution (yellow bars in Fig. 2) with the TEGa pressure which is characterized by the supply of GaP monolayer per cycle. If APDs grow straight up through the crystal, they typically have a rectangular shape with similar edge lengths in the  $[110]$ - and  $[\bar{1}\bar{1}0]$ -directions. [26] Such fourfold anisotropy is in fact slightly visible in the  $sS$  component of the rotational SHG anisotropy for sample FME1.30ML (yellow curve in Fig. 1 c)).

The STEM image of the CGM sample (Fig. 3 (b)) shows no APDs and, consequently, a small magnitude

of  $a_{sS}$ . In this growth mode, however, the formation of twins is favored as discussed in detail in Ref. 27. Such twin, which is sketched in Fig. 3 (d), can be clearly observed in the STEM image of the CGM sample. It gives rise to a two-fold anisotropy between the  $[\bar{1}\bar{1}0]$  and  $[110]$  directions because twins predominately form on Ga-terminated  $(111)$  A planes. [27, 28] This anisotropy is

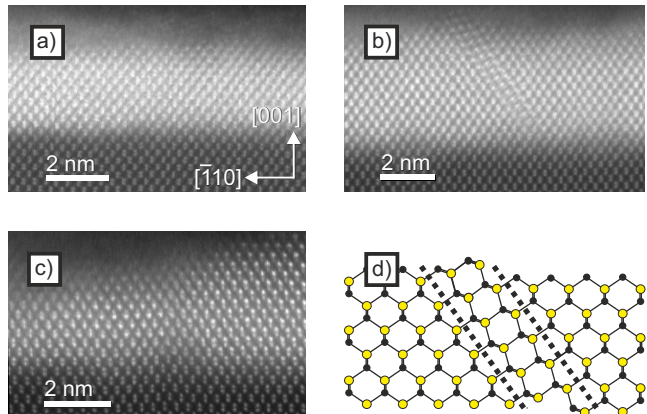


FIG. 3: (Color online) STEM images of the interface of (a) FME0.97ML, (b) CGM, and (c) FME1.30ML. (d) Scheme of twins in GaP. Ga (P) atoms are depicted by yellow (black) dots.

characterized by a large magnitude of  $b_{pP}^{(2)}$  (cyan/white bars in Fig. 2) for the CGM sample. In contrast,  $b_{pP}^{(2)}$  is comparable small for all FME samples.

The anisotropy for the  $pS$  polarization combination is characterized by the parameters  $c_{pS}^{(2)}$  and  $b_{pS}^{(4)}$  which are depicted by orange and red/white bars in Fig. 2, respectively. These parameters might be further indicators for the film quality. They show, however, no clear trend for the different growth modes and cannot be correlated to specific defects observed in STEM.

In summary we have shown that second-harmonic generation can be successfully used as a sensitive, non-invasive probe for the quality of the interface between thin films of GaP and Si(001). The rotational anisotropy of the second-harmonic intensity could be correlated to specific defects that form at different growth conditions in metal organic vaporphase epitaxy. In particular, the occurrence of antiphase domains and twins could be clearly identified. We propose to use this all-optical technique as an *in-situ* monitor of the growth process.

We gratefully acknowledge funding by the Deutsche Forschungsgemeinschaft through SFB 1083, project B5.

[1] Y. R. Shen, Annu. Rev. Phys. Chem. **40**, 327 (1989).  
 [2] T. F. Heinz, F. J. Himpsel, E. Palange, and E. Burstein, Phys. Rev. Lett. **63**, 644 (1989).

[3] T. F. Heinz, in *Nonlinear Surface Electromagnetic Phenomena*, edited by H.-E. Ponath and G. I. Stegeman (Elsevier Science Publishers B.V., Amsterdam, 1991), pp.

- 353–416.
- [4] G. A. Reider and T. F. Heinz, in *Photonic Probes of Surfaces*, edited by P. Halevi (Elsevier Science B.V., Amsterdam, 1995), pp. 415–70.
- [5] T. Stehlin, M. Feller, P. Guyotssonest, and Y. R. Shen, *Opt. Lett.* **13**, 389 (1988).
- [6] M. S. Yeganeh, J. Qi, A. G. Yodh, and M. C. Tamargo, *Phys. Rev. Lett.* **69**, 3579 (1992).
- [7] S. Liebich, M. Zimprich, A. Beyer, C. Lange, D. J. Franzbach, S. Chatterjee, N. Hossain, S. J. Sweeney, K. Volz, B. Kunert, and W. Stolz, *Appl. Phys. Lett.* **99**, 071109 (2011).
- [8] O. Supplie, M. M. May, G. Steinbach, O. Romanyuk, F. Grosse, A. Nägelein, P. Kleinschmidt, S. Brückner, and T. Hannappel, *J. Phys. Chem. Lett.* **6**, 464 (2015).
- [9] H. Kroemer, *J. Cryst. Growth* **81**, 193 (1987).
- [10] K. Volz, A. Beyer, W. Witte, J. Ohlmann, I. Nemeth, B. Kunert, and W. Stolz, *J. Cryst. Growth* **315**, 37 (2011).
- [11] A. Beyer, I. Nemeth, S. Liebich, J. Ohlmann, W. Stolz, and K. Volz, *J. Appl. Phys.* **109**, 083529 (2011).
- [12] A. Beyer, B. Haas, K. I. Gries, K. Werner, M. Luysberg, W. Stolz, and K. Volz, *Appl. Phys. Lett.* **103**, 032107 (2013).
- [13] A. Beyer, A. Stegmüller, J. O. Oelerich, J. Kakhaber, K. Werner, G. Mette, W. Stolz, S. D. Baranovskii, R. Tonner, and K. Volz, *Chem. Mater.* **28**, 3265 (2016).
- [14] K. Stépán, M. Dürr, J. Güdde, and U. Höfer, *Surf. Sci.* **593**, 54 (2005).
- [15] H. W. K. Tom, T. F. Heinz, and Y. R. Shen, *Phys. Rev. Lett.* **51**, 1983 (1983).
- [16] G. Lupke, *Surf. Sci. Rep.* **35**, 77 (1999).
- [17] K. Ishioka, K. Brixius, A. Beyer, A. Rustagi, C. J. Stanton, W. Stolz, K. Volz, U. Höfer, and H. Petek, *Appl. Phys. Lett.* **108**, 051607 (2016).
- [18] U. Höfer, *Appl. Phys. A* **63**, 533 (1996).
- [19] C. H. Lee, R. K. Chang, and N. Bloembergen, *Phys. Rev. Lett.* **18**, 167 (1967).
- [20] O. A. Aktsipetrov, A. A. Fedyanin, J. I. Dadap, and M. C. Downer, *Laser Phys.* **6**, 1142 (1996).
- [21] J. Qi, M. S. Yeganeh, I. Koltover, A. G. Yodh, and W. M. Theis, *Phys. Rev. Lett.* **71**, 633 (1993).
- [22] T. A. Germer, K. W. Kolasinski, J. C. Stephenson, and L. J. Richter, *Phys. Rev. B* **55**, 10694 (1997).
- [23] O. A. Aktsipetrov, A. A. Fedyanin, A. V. Melnikov, E. D. Mishina, A. N. Rubtsov, M. H. Anderson, P. T. Wilson, H. ter Beek, X. F. Hu, J. I. Dadap, and M. C. Downer, *Phys. Rev. B* **60**, 8924 (1999).
- [24] M. Lei, J. Price, W. E. Wang, M. H. Wong, R. Droopad, P. Kirsch, G. Bersuker, and M. C. Downer, *Appl. Phys. Lett.* **102**, 152103 (2013).
- [25] J. E. Sipe, D. J. Moss, and H. M. van Driel, *Phys. Rev. B* **35**, 1129 (1987).
- [26] K. Werner, A. Beyer, J. Oelerich, S. Baranovskii, W. Stolz, and K. Volz, *J. Cryst. Growth* **405**, 102 (2014).
- [27] S. L. J. O. W. S. A. Beyer, Igor Nemeth and K. Volz, *Journ. Appl. Phys.* **109**, 083529 (2011).
- [28] O. Skibitzki, F. Hatami, Y. Yamamoto, P. Zaumseil, A. Trampert, M. A. Schubert, B. Tillack, W. T. Masselink, and T. Schroeder, *J. Appl. Phys.* **111**, (2012).